

# Subtle Determinants of the Nucleocytoplasmic Partitioning of In Vivo-Transcribed RNase MRP RNA in *Xenopus laevis* Oocytes

SUNJOO JEONG-YU,<sup>1,2</sup> ALISON F. DAVIS,<sup>1</sup> AND DAVID A. CLAYTON<sup>3</sup>

*Department of Developmental Biology, Stanford University School of Medicine,  
Stanford, CA 94305-5427*

RNase MRP is a ribonucleoprotein originally identified on the basis of its ability to cleave RNA endonucleolytically from origins of mitochondrial DNA replication, rendering it a likely candidate for a role in priming leading-strand synthesis of mtDNA. In addition, a nuclear role for RNase MRP has been identified in yeast (*Saccharomyces cerevisiae*) ribosomal RNA processing. Consistent with a duality of function, RNase MRP has been localized to both mitochondria and nucleoli by in situ techniques. The RNA component of this ribonucleoprotein has been characterized from several different species. We previously cloned the gene for *Xenopus laevis* MRP RNA and showed that RNase MRP RNA is differentially expressed during amphibian development; in addition, the microinjected *X. laevis* RNase MRP RNA gene is correctly and efficiently transcribed in vivo. This article presents an analysis of the intracellular movement of in vivo-transcribed RNase MRP RNA in microinjected mature *X. laevis* oocytes. Although *X. laevis* MRP RNA is assembled into a ribonucleoprotein form and transported in an expected manner, human and mouse MRP RNAs exhibit markedly different transport patterns even though they are highly conserved in primary sequence. Furthermore, the only currently assigned protein (Th autoantigen) binding site in MRP RNA can be deleted without loss of nuclear export capacity. These results indicate that subtle determinants must exist for nucleocytoplasmic partitioning of this RNP and that the conserved Th autoantigen binding region appears unnecessary for the transit of in vivo-transcribed MRP RNA to the cytoplasm of mature *X. laevis* oocytes.

MRP RNA	<i>Xenopus laevis</i>	Th autoantigen	Export
---------	-----------------------	----------------	--------

RIBONUCLEOPROTEINS (RNPs) are an expanding group of RNA-protein complexes that have been implicated in diverse cellular processes. Of these, RNase MRP is an RNP that we have characterized in some detail in recent years. Most of our studies to date have focused upon the enzymatic properties of the holoenzyme (5,26,36). It has been established that both RNA and protein components of RNase MRP are required for cata-

lytic function (5). The gene for the RNA component of RNase MRP (MRP RNA) has been cloned from species as divergent as yeast and humans. MRP RNA is essential for viability in yeast cells (26,31) and the striking amount of sequence conservation over evolutionary time strongly suggests its importance in cellular function.

The originally described substrate for RNase MRP is a mitochondrial RNA sequence from the

Received July 26, 1995; revision accepted September 6, 1995.

<sup>1</sup>Equal contribution to this work.

<sup>2</sup>Current address: Department of Molecular Biology, College of Natural Sciences, Dankook University, Hannam-dong, Yongsan-gu, Seoul 140-714 Korea.

<sup>3</sup>Address correspondence to David A. Clayton.

origin of heavy-strand mitochondrial DNA replication (4). This enzyme has thus been hypothesized to provide RNA primers for the initiation of mitochondrial DNA replication by mitochondrial DNA polymerase. In addition, the multifunctional RNase MRP enzyme exhibits nonmitochondrial function in the nucleus (nucleolus), where a role in rRNA maturation has been established (7,30). Complete functional characterization of the RNase MRP enzyme *in vivo* remains an arduous task, based upon its proposed roles in these two distinct intracellular compartments, mitochondria and nucleoli (8).

There is mounting evidence that both small nuclear ribonucleoproteins (snRNPs) (e.g., U1, U2, U4, U5, U6, and U7) and small nucleolar ribonucleoproteins (snoRNPs) (e.g., U3, U8, U13, U14, U15, U22, RNase MRP) function in large processing complexes that process mRNAs and rRNAs, respectively (24). Functional RNPs require the correct assembly of RNA and protein components, an event that may occur in subcellular regions distinct from where they function (22). The spliceosomal snRNAs represent a class of RNAs that require a cytoplasmic maturation phase in which they acquire a hypermethylated m<sup>7</sup>G cap at their 5' end, associate with Sm proteins, and then reenter the nucleus as mature RNP particles. In contrast, it has been recently shown that at least one snoRNA (U3) acquires a m<sup>2,2,7</sup>G cap structure and is further processed into a mature form entirely within the nucleus (34). It is not yet clear whether this is generally true for other snoRNAs that function in nucleoli.

RNase MRP can be classified as an snoRNP by some criteria but not others. MRP RNA has a nonnuclear function; hence, it need not be retained and modified in the nucleus in all cases. Unlike most other snoRNAs, MRP RNA is not 5' capped, and thus does not have the characteristic hypermethylated cap structure. In addition, most snoRNAs bind the protein fibrillarin (18,19,38), whereas MRP RNA does not. The only protein that has been associated with MRP RNA in metazoans is the Th antigen, which is thought to associate with a portion of the 5' half of MRP RNA (40). Other protein components of RNase MRP have remained elusive, with the possible exception of *S. cerevisiae*, in which only a single MRP-specific polypeptide (SNM1) has been identified to date (32), along with one other protein (POP1), which also associates with RNase MRP's probable ancestral relative, RNase P (21).

In contrast, nuclear genes encoding the RNA component of RNase MRP have been readily

identified and cloned from several species. Previous studies involving either chemical probing strategies (37) or phylogenetic comparison (29) have analyzed proposed structural features of the RNA component of RNase MRP. These studies have permitted the construction of models representative of the likely secondary structure of this RNA, allowing speculation about potential interactions between the RNA and protein(s) and/or nucleic acid substrate moieties. This type of analysis has revealed several regions in which there exist extensive conservation between relatively divergent species. Some of the conserved regions display intrastrand complementarity, which are likely base-paired *in vivo*.

SnRNPs can shuttle between the nucleus and cytoplasm, where they function in the processing of pre-mRNA (27). Several nucleolar proteins also move between the nucleus and cytoplasm (3), these proteins presumably playing a role in ribosomal function by transporting ribosomal proteins, pre-rRNAs, and possibly certain snoRNPs. Many features of the nucleocytoplasmic trafficking of RNAs (and of RNPs) have been intensively studied and a few universal principles have been identified, mostly with respect to nuclear import mechanisms (15,25). In contrast, less is known concerning modes of export of RNAs and RNPs. Export of these moieties to the cytoplasmic space likely involves both negative signals (preventing nuclear exit) and positive signals (promoting cytoplasmic entry). It is generally accepted that the transit of RNAs from the nucleus to the cytoplasm and back is in some way protein mediated, via cognate proteins of the RNP complex itself as well as through proteins present in the nucleus, such as various protein components of the nuclear pore complex (12,25). We have employed *X. laevis* oocytes as an experimental system in which to begin to analyze *in vivo* some of the sequence and/or potential structural determinants of MRP RNA with regard to nucleocytoplasmic partitioning, an event that is most likely required for the proper assembly of nucleic acid and protein components, both of which characterize the functional RNase MRP holoenzyme.

## MATERIALS AND METHODS

### *Preparation of Oocytes and Microinjection*

To obtain oocytes for microinjection, ovarian sections were surgically removed from mature adult female frogs and then treated with collagenase (Sigma, type 1A) as previously described (2).

Oocytes were staged according to Dumont (11) and incubated in OR-2 buffer (39). Oocytes were manually defolliculated and then dissected into nuclear and cytoplasmic fractions in ice-cold J-buffer (70 mM NH<sub>4</sub>Cl, 7 mM MgCl<sub>2</sub>, 10 mM HEPES, 0.1 mM EDTA, 2.5 mM DTT, 10% glycerol, 1% polyvinylpyrrolidone) (33). For injection experiments, a 30-nl volume of either DNA (closed circular plasmid DNA) or RNA (in vitro transcribed RNA) was injected into either the cytoplasmic or nuclear compartments of stage VI oocytes. Injected plasmids included pXIMRP [genomic *X. laevis* MRP RNA gene (2)], pMRPSP [genomic mouse MRP RNA gene (6)], pMRPHU [genomic human MRP RNA gene (36)], and frog/mouse hybrid constructs pXpM, pMpX, pMX, and pXM (plasmid construction described in detail below). Ten to 50 ng/ $\mu$ l was injected into the nuclei (germinal vesicles) of stage VI oocytes; results obtained were similar with either concentration. Injection RNA (full-length mouse MRP RNA, 275 nt) was obtained by in vitro transcription of HphI-linearized pT7-275C (37) with T7 RNA polymerase. At least 20 oocytes were injected for each time point. Ten oocytes were dissected for Northern blot analysis; total RNA from two oocytes was loaded per lane of an 8% polyacrylamide/8 M urea gel. In all Northern blot experiments, uninjected oocyte controls were analyzed in parallel. Ten oocytes were analyzed for immunoprecipitation 20 h postinjection.

#### *Hybrid and Deletion Plasmid Constructs*

Hybrid plasmids were constructed using the method of overlap extension mutagenesis (14), in which mutated regions are created by first generating two DNA fragments (through PCR) with overlapping ends; the mutation is created in a second PCR reaction, using the most 5' and 3' primers from each of the first two PCR reactions to amplify the overlapping region. In general, PCR reactions contained 50 mM KCl, 10 mM Tris-Cl (pH 8.3), 1.5 mM MgCl<sub>2</sub>, 0.1% gelatin, 1.5 mM dNTPs (375  $\mu$ M each dGTP, dATP, dTTP, dCTP), 500 nM each 5' and 3' primers, 1  $\mu$ g template DNA, and 2.5 units Amplitaq polymerase (Perkin-Elmer) in a final reaction volume of 100  $\mu$ l. Samples were overlaid with light mineral oil and subjected to 20 cycles of denaturation (5 min, 94°C), annealing (2 min, 48°C), and polymerization (3 min, 72°C) in a thermocycler (Hybaid). PCR products were then analyzed by standard agarose gel electrophoretic methods and subsequently gel purified. Blunt ends in final PCR

products (representing mutated regions) were generated with Klenow polymerase and then cloned into pBluescript-KS(-) (Stratagene) through blunt-end ligation.

Specifically, hybrid constructs (pXpM, pMpX, pXM, and pMX) were generated as follows. To create plasmid pXpM, the first DNA fragment was obtained by amplifying template DNA pXLMRP (genomic *Xenopus laevis* MRP RNA clone) (2) with oligo 5-2 (5' primer): 5'-CGCGGA TCCAAGTTTGGCAGACTGTT-3' and oligo 9 (3' primer): 5'-GAGCGAGCTAATGAACCCA TCCCCCTTC-3'. The second DNA fragment was generated through amplification of template DNA pMRPSP (genomic mouse MRP RNA clone) (6) with oligo 10 (5' primer): 5'-GGG TTCATTAGCTCGCTCTGAAGGCCTG-3' and oligo 8-2 (3' primer): 5'-CCGGAATTCAATCC CAGCACTCGGGA-3'. After gel purification, the products of the first two PCR reactions were fused by amplification of the overlapping region with oligos 5-2 and 8-2 (5' and 3' primers, respectively). Plasmid pMpX was created by first amplifying template DNA pMRPSP with oligo 1-2 (5' primer): 5'-CGCGGATCCAAGGCGCAGACA CAAGC-3' and oligo 11 (3' primer): 5'-AAT GCCTACGCCTTAACCTTCTAGGCGCGA - 3'. The second DNA fragment was generated by amplifying template DNA pXIMRP with oligo 12 (5' primer): 5'-AGTTAAGGCGTAGGCATTCTGA AGACCTG-3' and oligo 4-2 (3' primer): 5'-CCG GAATTCTTTAACCATGATGCAGG-3'. After gel purification, the products of the first two PCR reactions were fused by amplification of the overlapping region with oligos 1-2 and 4-2 (5' and 3' primers, respectively). Construct pMX was created by generating the first DNA fragment by amplifying template DNA pMRPSP with oligo 1-2 (5' primer) and oligo 2 (3' primer): 5'-ACGCCATATGTGCACGCGGCCATC-3' and the second DNA fragment with template DNA pXIMRP amplified with oligo 4-2 (5' primer) and oligo 3 (3' primer): 5'-CGTGCACATATGGCG TGCAATAAT-3'. After gel purification, the products of the first two PCR reactions were fused by amplification of the overlapping region with oligos 1-2 and 4-2 (5' and 3' primers, respectively). Finally, plasmid pXM was constructed by generating the first DNA fragment through amplification of template DNA pXLMRP with oligo 5-2 (5' primer) and oligo 6 (3' primer): 5'-TACGCGGGTAGCGCACGGCACTT-3'. The second fragment was created by amplifying template DNA pMRPSP with oligo 8-2 (5' primer) and oligo 7 (3' primer): 5'-TGCGCTACCGCG

CGTAGACTTCC-3'. After gel purification, the products of the first two PCR reactions were fused by amplification of the overlapping region with oligos 5-2 and 8-2 (5' and 3' primers, respectively). Hence, plasmids pMRPSP, pXpM, and pMX contain the mouse MRP RNA transcription start site, and plasmids pXIMRP, pMpX, and pXM contain the frog transcription start site. All introduced mutations (hybrid regions) were confirmed by sequencing using the dideoxy chain-termination method with Sequenase (United States Biochemical).

Deletion constructs p $\Delta$ Th1 and p $\Delta$ Th2 were derived from pXLMRP. p $\Delta$ Th1 was created by removing a BsiWI-StyI fragment from pXIMRP, and represents a 34-nt deletion (nt 34–67) that encompasses most of the inferred Th binding site. p $\Delta$ Th2 was constructed by removing a BbsI-BsiWI fragment from pXLMRP and represents a 14-nt deletion (nt 20–33) in this region of the RNA.

#### RNA Analysis and Preparation of Probes

Northern blots were performed with digoxigenin-labeled probes using the Genius chemiluminescent detection kit (Boehringer Mannheim) as previously described (2). *X. laevis* MRP RNA was detected with either an RNA or an oligonucleotide probe. An antisense MRP RNA probe was obtained via in vitro transcription of XhoI-digested plasmid pXLMU (2) with T7 RNA polymerase. The 5' MRP oligonucleotide probe, complementary to nucleotides 65–110 of *X. laevis* MRP RNA, was 3' end labeled with digoxigenin-11-ddUTP and terminal transferase. In vitro- or in vivo-transcribed mouse MRP RNA was detected with 3' end-labeled oligo 4 (37). In vivo-transcribed human MRP RNA was detected by linearizing plasmid PCRHU [a BamHI-MscI fragment encompassing the coding region of the human MRP RNA gene cloned into the PCRII vector (Stratagene)] with MscI followed by in vitro transcription with T7 RNA polymerase to generate an antisense probe. Immunoprecipitated RNAs were detected with Northern blot analysis, as described previously (2). Primer extension analysis was performed essentially as previously described (28), using oligos SM2 (5'-CCGGCG ACTTCCCTAGG-3') and XLPE (5'-AG CAGGGCGGGATTATT-3'), to determine the 5' ends of in vivo-transcribed RNA from injected plasmids pMRPSP, pXpM, and pMX (oligo SM2) and pXIMRP, pXM, and pMpX (oligo XLPE), respectively. Briefly, primers were end labeled

with polynucleotide kinase and 1 pmol of the radioactive probe was coprecipitated with RNA from each reaction with ethanol. The pellet was resuspended in 4.5  $\mu$ l of 550 mM Tris-Cl (pH 8.3), 450 mM KCl, incubated at 75°C for 10 min, then cooled to 43°C over 1–2 h. After annealing primer and RNA, the reaction volume was increased to a final volume of 50  $\mu$ l containing 50 mM Tris-Cl (pH 8.3), 40 mM KCl, 8 mM MgCl<sub>2</sub>, 1 mM DTT, 200  $\mu$ M nucleoside triphosphates, and MMuLV reverse transcriptase (10 units). Primers were extended for 1 h at 43°C. Primer-extended RNA was phenol-chloroform extracted and ethanol precipitated. RNA pellets were denatured for 5 min at 95°C, chilled on ice, then loaded onto a 6% polyacrylamide-7 M urea sequencing gel. Primer XLPE is complementary to nt 124–140 of *X. laevis* MRP RNA, and primer SM2 is complementary to nt 61–79 of mouse MRP RNA, yielding 140 nt and 79 nt primer-extended products, respectively.

## RESULTS

### *Nucleocytoplasmic Partitioning of Heterologous MRP RNAs in X. laevis Oocytes*

We previously showed that genomic *X. laevis* MRP DNA is correctly transcribed in mature *X. laevis* oocytes (2) and have recently observed that this in vivo-transcribed RNA is detectable within the oocyte cytoplasm within several hours postinjection of the *X. laevis* MRP RNA gene (10). Based upon the marked degree of sequence conservation of MRP RNA between species (29), we were interested in whether or not *X. laevis* oocytes were capable of transcription and/or transport of heterologous MRP RNAs. Indeed, recent studies have demonstrated that heterologous snRNA-encoding genes are transcribed and transported in *X. laevis* oocytes (33). To this end, we observed efficient transcription of a microinjected human MRP RNA genomic clone, followed by appearance of the in vivo-transcribed human MRP RNA in the cytoplasm (Fig. 1). The time course of nuclear-to-cytoplasmic partitioning of this RNA was not distinguishable from that of the cognate *X. laevis* MRP RNA (Fig. 3A). Interestingly, at later time points (e.g., 24 h, Fig. 1, lane 12, asterisk), a smaller hybridizing species (110 nt) is detectable in the cytoplasmic fraction. This may represent the 108-nt species of human MRP RNA identified previously (36).

We extended our interspecies comparison of

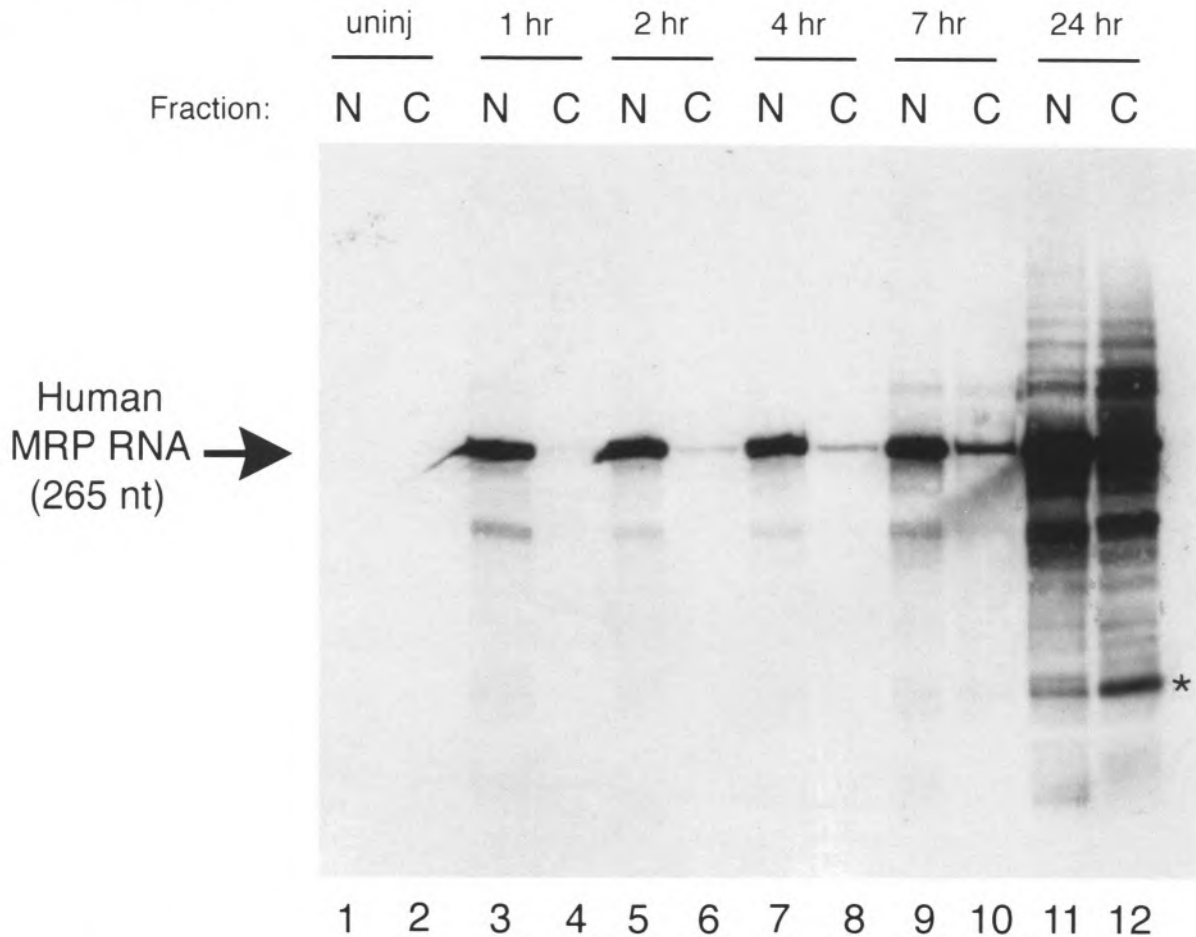


FIG. 1. Human MRP RNA is transcribed and exported in *X. laevis* oocytes. Genomic human MRP DNA was injected into the germinal vesicles (nuclei) of mature *X. laevis* oocytes (see Materials and Methods), and *in vivo*-transcribed RNA was detected by Northern analysis. Nuclear (N) or cytoplasmic (C) fractions of injected oocytes were manually isolated from uninjected (lanes 1, 2), or injected (lanes 3–12) oocytes at the indicated times postinjection. Total RNA from two oocytes was loaded per lane of an 8% polyacrylamide-8 M urea gel. After transfer to a nylon membrane, RNAs were hybridized with a digoxigenin-labeled *in vitro*-transcribed antisense human MRP RNA probe (see Materials and Methods) and visualized with chemiluminescence detection of the probe. Full-size human MRP RNA is 265 nt (36). Faster migrating species are presumably degradation products of the full-length MRP RNA; one of these (\*) may represent a previously identified 108 nt form of human MRP RNA (36). Note that the human antisense probe does not recognize the endogenous *X. laevis* MRP RNA (277 nt) (2) in uninjected (lanes 1, 2) or injected (lanes 3–12) oocyte fractions.

RNase MRP RNA transcription and transport with mouse MRP RNA, as RNase MRP isolated from mouse cells has been extensively characterized (4,5,16). Although microinjected genomic mouse DNA encoding MRP RNA was effectively transcribed, *in vivo*-transcribed mouse MRP RNA was incapable of nucleocytoplasmic partitioning (Fig. 2A), as was *in vitro*-transcribed mouse MRP RNA. Immunoprecipitation with the anti-Th autoantiserum was used to analyze the fate of the uncomplexed (free) RNA (Fig. 2B, anti-Th immunoprecipitation supernatant) as well as the complexed (at least with the Th antigen) MRP RNP (Fig. 2C, anti-Th immunoprecipitation pellet)

after injection of *in vitro*-transcribed mouse MRP RNA into either the nucleoplasmic or cytoplasmic spaces of the oocyte. It is clear that none of the RNA injected into the nucleus could be subsequently detected in the cytoplasm (Fig. 2B, lanes 1 and 2); however, this is not attributable to instability of the cytoplasmic form because MRP RNA injected into the cytoplasm of nucleated or enucleated cells was not significantly degraded (Fig. 2B, lanes 3 and 4). This *in vitro*-transcribed mouse MRP RNA was properly assembled with cognate proteins, as demonstrated by immunoprecipitation with Th autoantiserum (Fig. 2C, lane 1), suggesting that the *in vitro*-transcribed mouse MRP

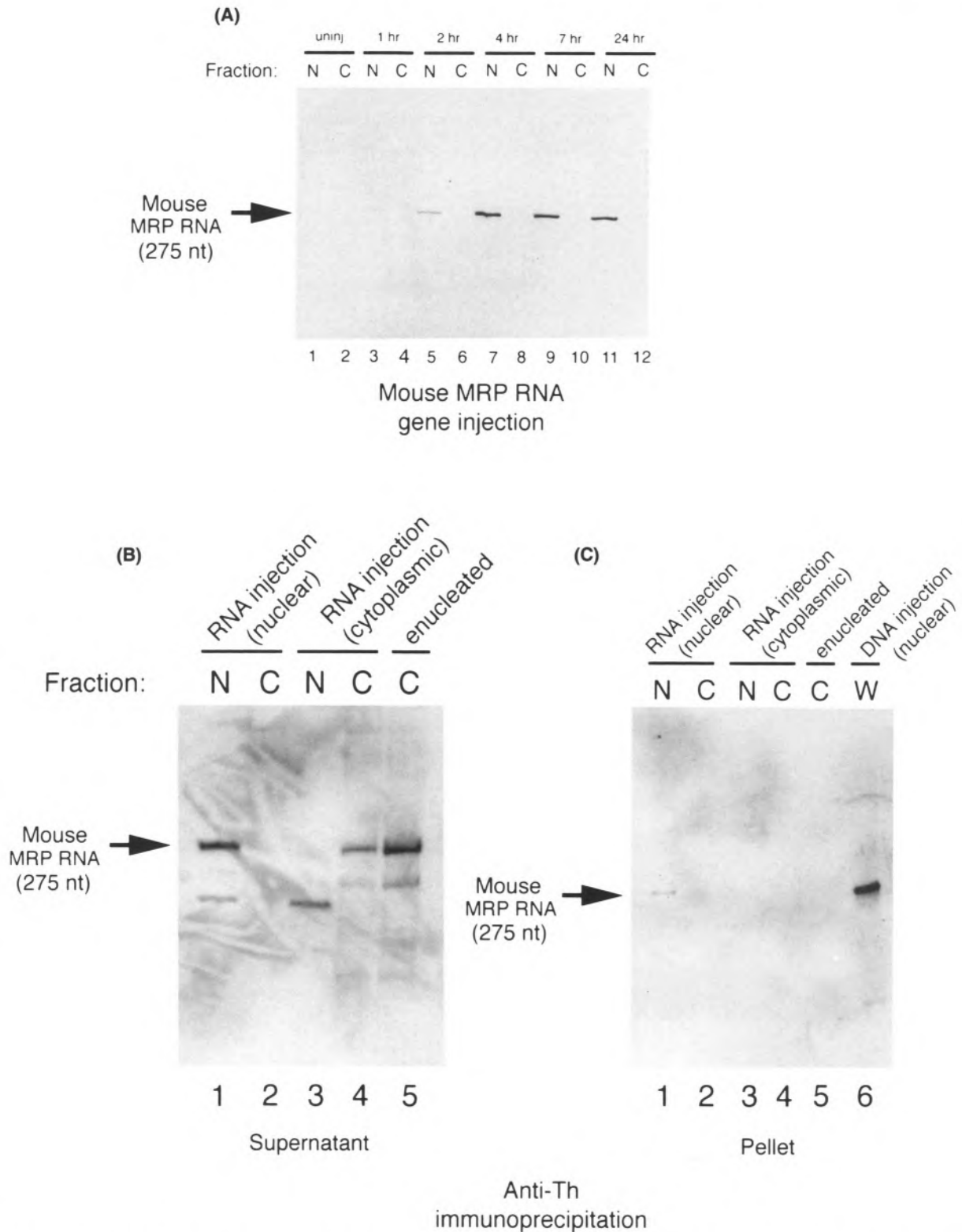


FIG. 2. Mouse MRP RNA is transcribed but not transported to the cytoplasm of *X. laevis* oocytes. Northern blot analysis was performed as in Fig. 1, with an oligonucleotide probe that recognizes mouse MRP RNA (see Materials and Methods). (A) Genomic mouse MRP DNA was injected into the nuclei of *X. laevis* oocytes, and in vivo-transcribed mouse MRP RNA was detected at the indicated times postinjection, as described in Materials and Methods. Full-length mouse MRP RNA is 275 nt (6). (B, C) In vitro-transcribed mouse MRP RNA was injected into either the nucleus (B, lanes 1, 2; C, lanes 1, 2) or cytoplasm (B, lanes 3, 4; C, lanes 3, 4) of either whole or enucleated (B, lane 5; C, lane 5) mature *X. laevis* oocytes. Nuclear (N) or cytoplasmic (C) fractions were manually isolated after 20 h, and total RNA was isolated, then immunoprecipitated with anti-Th antiserum (2). The immunoprecipitated pellet is shown in (C) and the nonimmunoprecipitated supernatant (representing uncomplexed RNA) is shown in (B). In vivo-transcribed mouse MRP RNA (from two whole oocytes, W) is shown for size comparison (C, lane 6).

RNA is not grossly defective structurally. These results also demonstrate that at least the association of MRP RNA with one protein of the RNP complex (the Th antigen) can occur readily inside the nucleus but not in the oocyte cytoplasm.

To determine whether transport of frog MRP RNA could be affected in *trans* by mouse MRP RNA, coinjection experiments were performed in which both plasmids were injected together into oocytes. Subsequently, *in vivo* transcript production of each species' MRP RNA was monitored in parallel with each cognate probe (Fig. 3A, B). The

results indicate that each RNA species behaves independently of the other, suggesting that the two MRP RNAs do not share the same transport machinery. This experiment also demonstrates that any existing nuclear retention mechanism was not overwhelmed, because even in the presence of overexpressed frog MRP RNA, mouse MRP RNA still fails to enter the cytoplasm. In addition, control experiments demonstrated the exclusively nuclear location of endogenous U6 RNA in the same 24-h postinjected samples in which *X. laevis* MRP RNA was present in approximately equal amounts

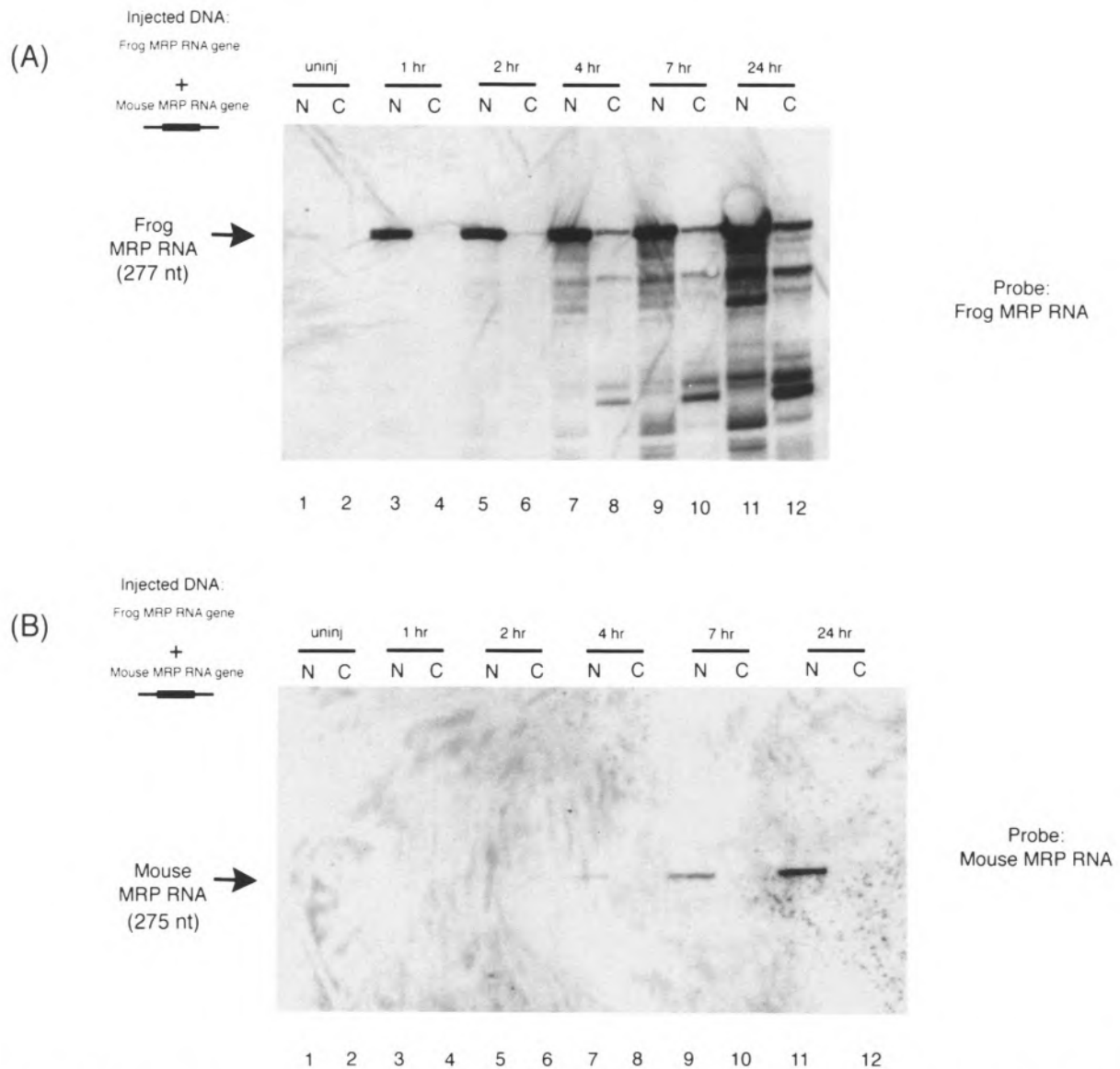
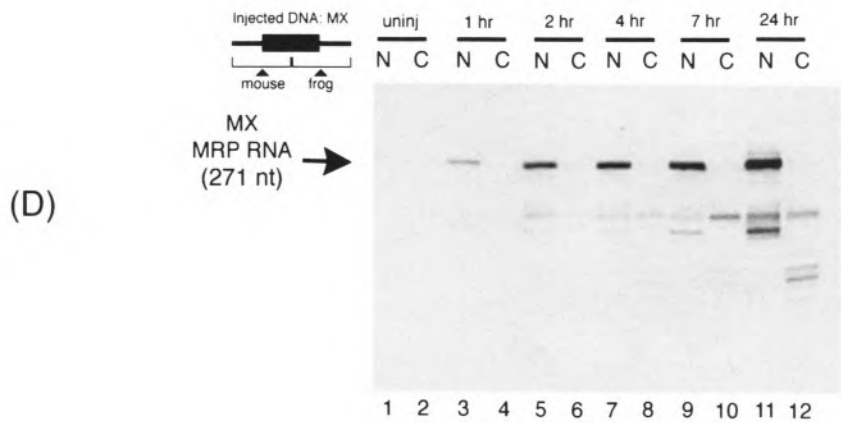
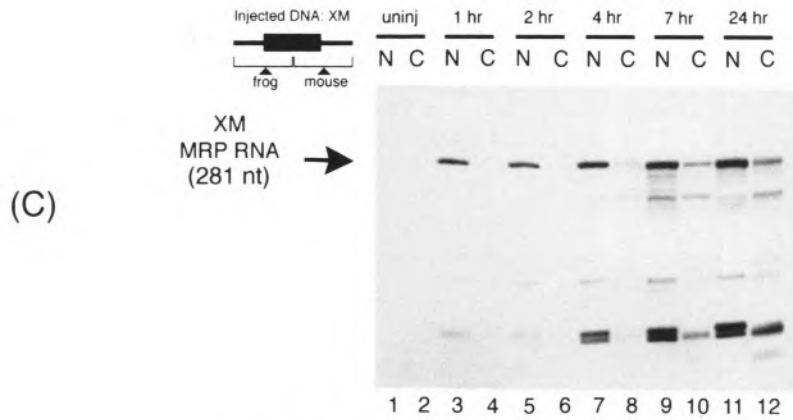
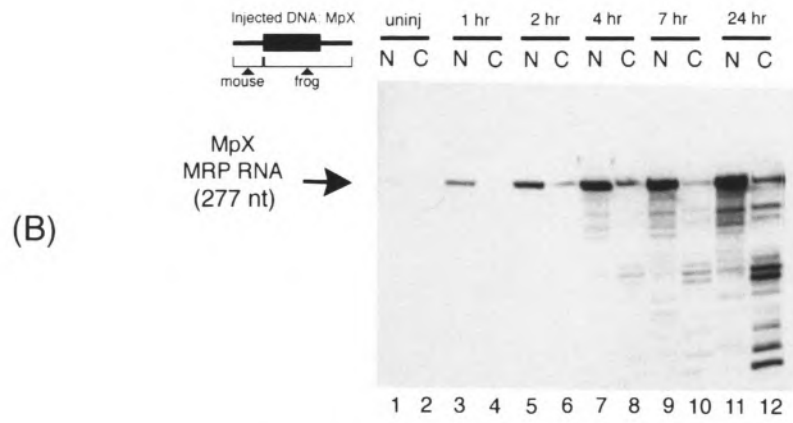
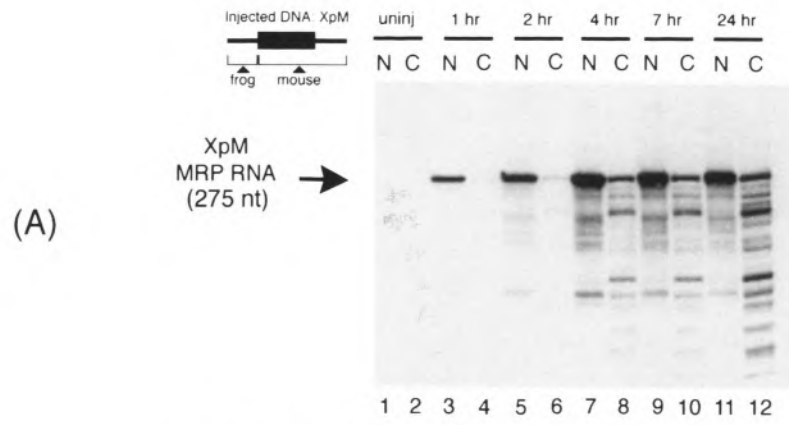


FIG. 3. In vivo-transcribed mouse and frog MRP RNA behave independently during coinjection. Oocytes were injected with both genomic mouse MRP DNA (50 ng/ $\mu$ l) and genomic *X. laevis* MRP DNA (20 ng/ $\mu$ l), in a total volume of 30 nl. In vivo-transcribed mouse MRP RNA or frog MRP RNA was detected by Northern analysis after the indicated times postinjection, as in Fig. 1, using each species' cognate probe (see Materials and Methods).





in nuclear and cytoplasmic oocyte fractions (data not shown). Collectively, these data argue against the possibility of any passive nuclear leakage phenomenon.

*The 5' Region of Mouse MRP RNA Is Defective in the Context of the Mouse Promoter Sequence*

We thus sought to identify regions of the mouse MRP RNA molecule that may be important for nuclear exit and/or cytoplasmic entry. We made hybrid plasmid constructs that contained regions of mouse and/or frog MRP RNA when transcribed *in vivo* (Fig. 4). Interestingly, replacement of the mouse promoter with the frog promoter (pXpM) rendered the mouse MRP RNA capable of nuclear exit (Fig. 4A); in fact, the phenotype approached that of the injected wild-type frog MRP RNA gene (Fig. 3A). However, mouse promoter sequences *per se* appear not to be entirely responsible for the observed mouse-specific defect, because swapping the frog promoter with its mouse counterpart (pMpX) slightly hampered, but did not prohibit, the nucleocytoplasmic partitioning of frog MRP RNA (Fig. 4B).

It is possible that transcription (or cotranscriptional processing) is somehow coupled to export. To investigate the potential importance of the transcriptional start site, plasmids were constructed that "swapped" the 5' and 3' portions of frog and mouse MRP RNA genes. These two constructs therefore represent the natural coupling of the cognate promoter and 5' start site of each species of MRP RNA. *In vivo*-transcribed MRP RNA representing 5' frog gene sequences upstream of 3' mouse sequence (pXM, driven by the frog MRP RNA promoter) was basically indistinguishable from wild-type frog sequence (compare Fig. 4C to Fig. 3A). However, surprisingly, MRP RNA containing 5' mouse sequence and 3' frog sequence (pMX) behaved identically to wild-type mouse MRP RNA; this version of MRP RNA (driven by the mouse MRP RNA promoter) did not exit the nucleus (Fig. 4D). These results suggest that a portion of the 5' mouse MRP RNA

sequence is somehow deficient with respect to transportability to the cytoplasm, but only in the context of the heterologous mouse promoter, because the frog promoter can by some means overcome this defect.

It is conceivable that the mouse promoter defines the mouse MRP RNA 5' end in a manner insufficient to direct this RNA out of the nucleus. As a first step to determine whether the observed defects in nucleocytoplasmic movement might be the result of an impaired 5' end, we performed primer extension analysis with the MRP RNA variants that were prohibited from nuclear exit. No obvious defects were noted in comparing the *in vivo* 5' end production of defective MRP RNAs (M and MX, Fig. 5, lanes 2, 3, and 4, respectively) with unaffected hybrid RNAs (MpX and XpM, Fig. 5, lanes 6 and 5, respectively; XM, data not shown) or with wild-type frog MRP RNA (X, Fig. 5, lane 1). In all cases, the expected 140-nt or 79-nt species (see the Materials and Methods section) was apparent, reflecting the published transcription start sites of frog and mouse MRP RNAs, respectively. The apparent disproportionate amount of RNA between lanes results from the fact that different relative amounts of *in vivo*-transcribed MRP RNA were loaded per lane (each representing different times of *in vivo* transcription), although the total amount of RNA loaded (5  $\mu$ g) was constant between lanes. The observed primer-extended products reflect the previously mapped 5' ends of both mouse (6) and frog (2) MRP RNAs. Interestingly, one of the regions harboring the little sequence divergence that exists between mouse and either human or frog MRP RNAs lies in the most 5' region of the molecule; that is, the extreme 5' regions of human and frog MRP RNA are more similar by virtue of sequence (and predicted structure) than that of mouse and frog MRP RNAs. It is thus possible that the mouse promoter is incapable of conferring a proper 5' end structure with mouse MRP RNA, and that these defects are too subtle to detect easily by sequence alone.

FACING PAGE

FIG. 4. Frog-mouse MRP RNA hybrid constructs reveal subtle features of nucleocytoplasmic partitioning in *X. laevis* oocytes. Hybrid constructs (XpM, MpX, XM, or MX) (see Materials and Methods) were injected into the nuclei of mature *X. laevis* oocytes. *In vivo*-transcribed hybrid RNAs were detected by Northern analysis after the indicated times postinjection, as in Fig. 1, with the appropriate probes. Manually isolated nuclear (N) and cytoplasmic (C) fractions are shown. Full-length hybrid RNAs are indicated with arrows. Smaller RNA species presumably represent degraded forms of MRP RNA that are most prominent several hours postinjection. (A) *In vivo*-transcribed XpM MRP RNA. (B) *In vivo*-transcribed MpX MRP RNA. (C) *In vivo*-transcribed XM MRP RNA. (D) *In vivo*-transcribed MX MRP RNA.

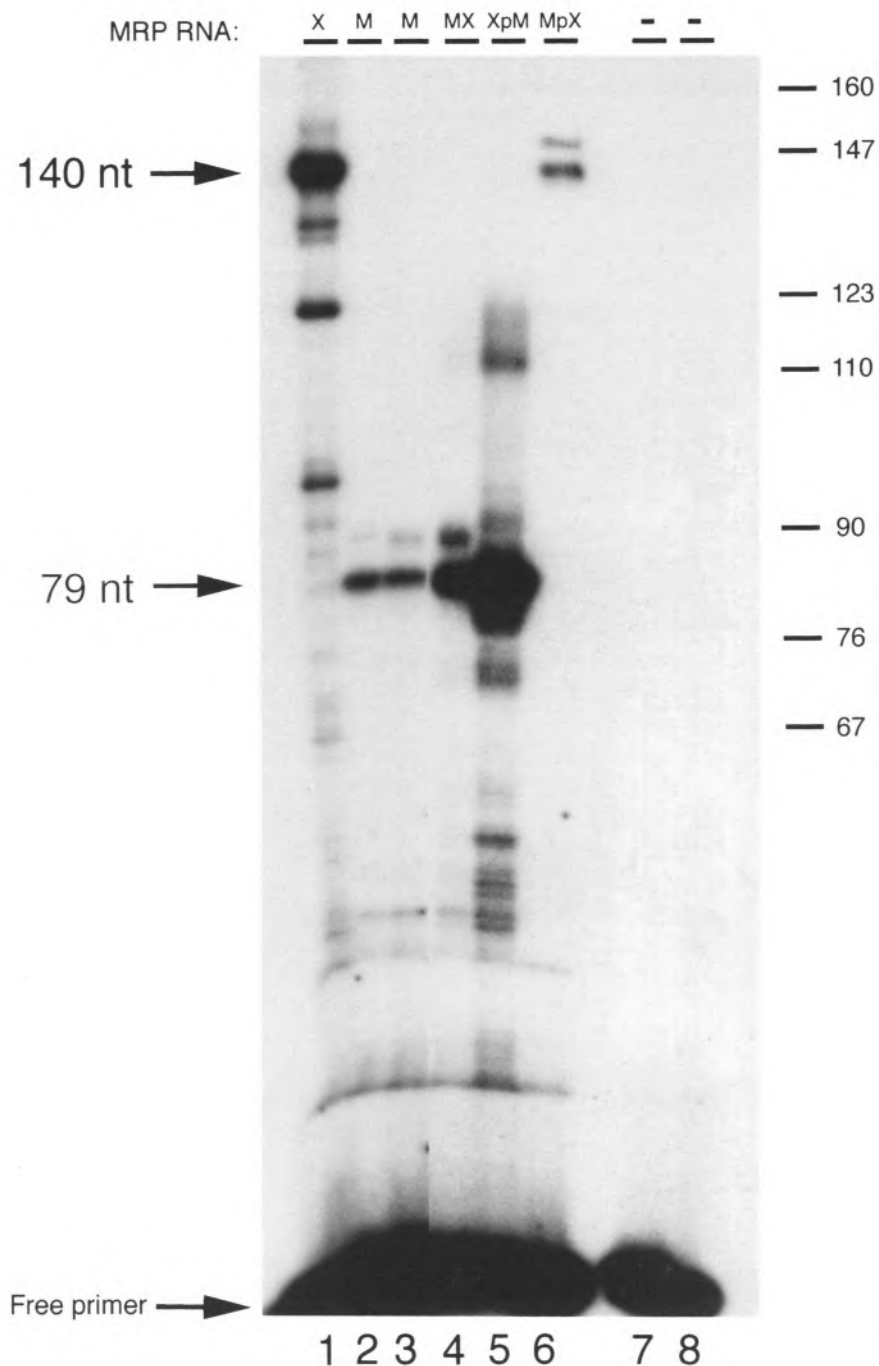
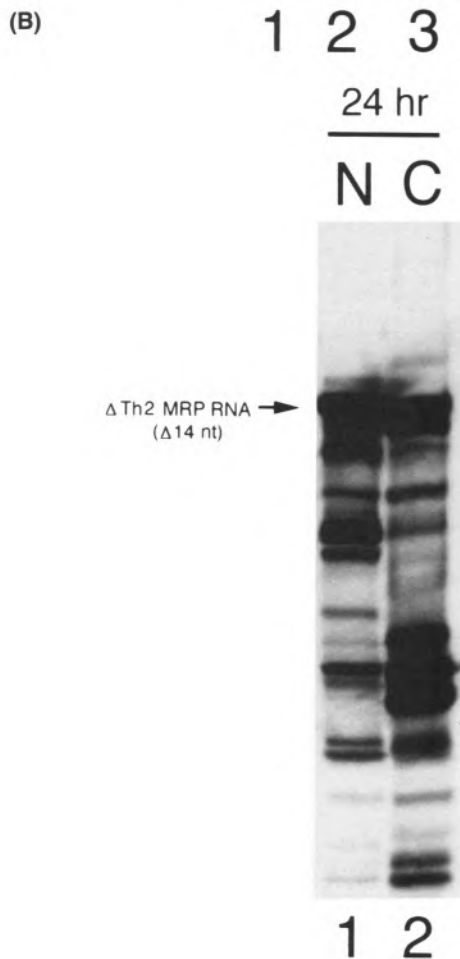
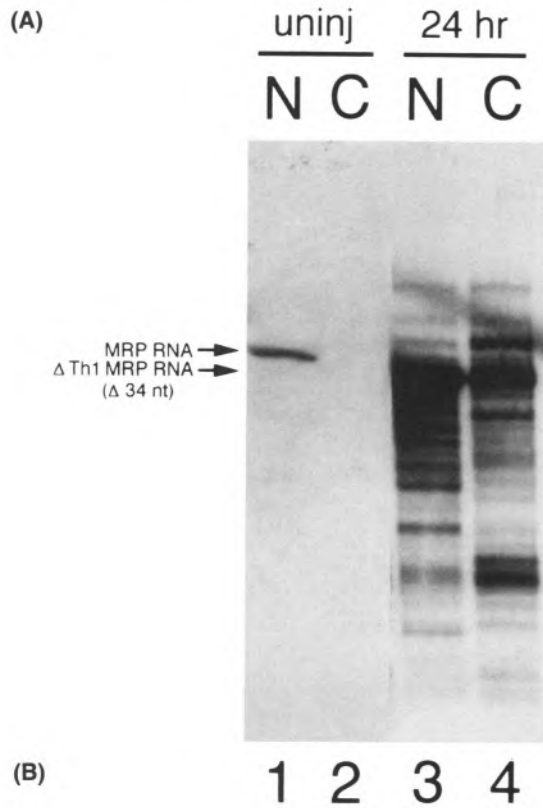


FIG. 5. Primer extension analysis of hybrid constructs reveals normal 5' ends of in vivo-transcribed MRP RNAs. Primer-extended RNAs ( $5 \mu\text{g}/\text{lane}$ ) were resolved on a 6% polyacrylamide-7 M urea high-resolution gel; free primers are indicated. Total RNA was isolated from injected oocytes. In vivo-transcribed X, M, MX, XpM, and MpX MRP RNAs, each represent  $5 \mu\text{g}$  total RNA from 4.5, 24, 24, 4.5, 24, and 2 h postinjection oocytes, respectively, and are shown in lanes 1-6, respectively. Reactions performed in the absence of RNA are shown in lanes 7 and 8.



*The Inferred Th Autoantigen Binding Region Is Not Required for Nucleocytoplasmic Partitioning of MRP RNA*

The only protein that has been associated with MRP RNA from all vertebrate species examined to date is the Th autoantigen. We observed that nonexportable mouse MRP RNA nevertheless associated with the *X. laevis* Th protein, as assessed by immunoprecipitation (Fig. 2). From these results, we predicted that this region might be unnecessary for the transport of MRP RNA from the nucleus to the cytoplasm of oocytes. To test this, we constructed two deletion mutations of *X. laevis* MRP RNA (see the Materials and Methods section). These two constructs represented 14-nt and 34-nt deletions within the highly conserved cage region (27), which is the inferred Th autoantigen binding region (40). Neither of these deletions had any effect on the ability of MRP RNA to enter the cytoplasm (Fig. 6A, B). The appearance of higher mobility species most likely represents degradation products of the full-length MRP RNA, which are typically apparent after 24 h in *in vivo*-transcription experiments (Figs. 1, 3, and 4).

DISCUSSION

We employed *X. laevis* oocytes as a system to characterize some of the determinants of nucleocytoplasmic trafficking of the ribonucleoprotein RNase MRP. Our results indicate that there are likely subtle determinants dictating the intracellular movement and maturation of the RNA component of the ultimate RNP particle. Because a limited portion of MRP RNA functions in a nonnuclear location, its maturation pathway may be inherently different from that of other snoRNAs, which are thought to function solely within nuclear boundaries and may undergo maturation there as well, as has been shown for U3 snoRNA (34). We observed that *in vivo*-transcribed MRP RNA from different species is differentially han-

FIG. 6. The Th antigen-binding region is dispensible for the nucleocytoplasmic transit of *X. laevis* MRP RNA. Deletion constructs (ΔTh) (see Materials and Methods) were injected into mature *X. laevis* oocytes, and *in vivo*-transcribed RNA (24 h postinjection) was detected by Northern analysis, as in Fig. 1. (A) ΔTh1. Endogenous *X. laevis* MRP RNA (277 nt) is shown for comparison; ΔTh1 expectedly migrates slightly faster than endogenous MRP RNA because it is 34 nt shorter (compare lanes 3 and 4 with lanes 1 and 2). (B) ΔTh2. In each case, note approximately equal amounts of ΔTh MRP RNA in nuclear (N) and cytoplasmic (C) fractions.

dled by the *X. laevis* nucleocytoplasmic transport machinery (Figs. 1 and 2). The surprising finding that human and mouse MRP RNA behave differently in frog cells implies that there must exist very selective parameters that govern nucleocytoplasmic movement in these cells, because these RNAs are 81% identical at the primary sequence level (29). However, this result does not necessarily indicate that the mechanisms of transport of human and mouse MRP RNAs are fundamentally different in the context of human and mouse cells, respectively.

The predicted secondary structure of the MRP RNA molecule suggests that the 5' and 3' ends of MRP RNA are extensively base-paired (29). This may contribute to an important secondary structure that permits MRP RNA to adopt a correct conformation for intracellular transit. In this study, mouse MRP RNA (either in vitro or in vivo transcribed) was incapable of nucleocytoplasmic movement (either export from or import into the nucleus). In all cases (except for one, as discussed below), the mouse promoter was generally transcriptionally competent in frog cells, yet unable to sponsor synthesis of an RNA molecule that was capable of exiting the oocyte nucleus, even under conditions of overexpression, in which homologous forms of MRP RNA appear in the cytoplasm after a period of a few hours. The exceptional case was the frog MRP RNA gene driven by the mouse promoter, which exhibited a modest ability to enter the oocyte cytoplasm in comparison to wild-type frog MRP RNA. It remains unclear what type of mechanism permits this version of MRP RNA to exit the nuclear compartment of frog cells to a limited extent.

An interesting possibility is that transcription of MRP RNA is somehow coupled to export. To date, little is known concerning the transcriptional regulation of RNase MRP RNA genes other than the reported requirement of 90 nt of DNA immediately upstream of the transcription start site of the human MRP RNA gene for transcription in vitro (41). Clearly, our results do not support a mechanism in which accurate transcription alone is necessary and sufficient for nucleocytoplasmic partitioning in *X. laevis* oocytes. However, it is possible that cotranscriptional events might impart structural features to the RNA molecule that are essential for the association of certain export-related proteins.

In the case of other RNA types [mRNA (9), tRNA (42), rRNA (1)], energy-dependent, saturable export processes have been previously de-

scribed. There is mounting evidence that although certain mechanistic commonalities may exist, it is most probable that nuclear export of different types of RNA is mediated by specific factors for each class of RNA (15). A recent study showed that the RNA components of the Ro/SS-A autoantigen (Y RNAs) associate with at least some of their cognate protein components within the *X. laevis* oocyte nucleus (33). Following assembly, mature Ro RNP particles are rapidly exported to the cytoplasm (33).

To date, the only protein that has been shown to associate with MRP RNA across species boundaries is the Th autoantigen (13). Antisera from patients with autoimmune diseases such as systemic lupus erythematosus are immunoreactive against certain RNPs, including RNase MRP and RNase P. Mutational analysis of the human MRP RNA component has identified the likely region of association of this RNA with the Th protein(s) (40). Our results with mouse MRP RNA (either in vitro or in vivo transcribed) (Fig. 2) suggest that, as for the Ro RNP, MRP RNA assembly with the Th autoantiserum occurs within the confines of the *X. laevis* oocyte nucleus. Although assembly of the mouse MRP RNA with at least the Th antigen (as assessed by immunoprecipitation) appeared normal in oocyte nuclei, nonetheless this RNA could not exit the nucleus (Fig. 2). From these results, we infer that the Th autoantigen is not sufficient for nuclear exit of the RNase MRP RNP. Other data to support this conclusion include the fact that neither of two different deletion constructs (encompassing, and thereby removing, the inferred Th antigen binding region correlate in *Xenopus* MRP RNA) was retained in the oocyte nucleus (Fig. 6). These results suggest that this region is dispensible for nucleocytoplasmic transit.

We note that the localization of MRP RNA to the cytoplasm as reported here does not address directly the issue of mitochondrial localization. Although a significant number of in vitro studies of RNase MRP have documented cleavage of relevant mitochondrial RNA sequences (35), subcellular fractionation protocols have shown that only a very limited amount of MRP RNA is isolated in purified mitochondrial fractions (5,17,35). More recently, in situ hybridization techniques have been employed to test directly for MRP RNA presence in mitochondria (10,20). In addition, MRP RNA detection has served as a control in a careful and systematic in situ analysis of selected RNA polymerase III transcripts (23). In these cases MRP RNA was either assigned as mitochon-

drial in location (20) or the results were compatible with this conclusion (10,23).

Precise characterization of the RNase MRP holoenzyme in the *X. laevis* oocyte system awaits the identification of the full complement of MRP-associated polypeptides. It is possible that distinct protein components might direct RNase MRP RNA to different cellular compartments, in which case use of *X. laevis* oocytes may provide a tool to begin to resolve such pathways.

#### ACKNOWLEDGEMENTS

We thank members of our laboratory for useful comments and suggestions throughout the course of this work, especially Dr. G. S. Shadel for critical reading of the manuscript. This work was supported by grant GM-33088-25 from the National Institute of General Medical Sciences (to D.A.C.). A.F.D. is supported by a postdoctoral fellowship from the Evelyn Neizer Fund.

#### REFERENCES

1. Bataillé, N.; Helser, T.; Fried, H. M. *J. Cell Biol.* 111:1571-1582; 1990.
2. Bennett, J. L.; Jeong-Yu, S.; Clayton, D. A. *J. Biol. Chem.* 267:21765-21772; 1992.
3. Borer, R. A.; Lehner, C. F.; Eppenberger, H. M.; Nigg, E. A. *Cell* 56:379-390; 1989.
4. Chang, D. D.; Clayton, D. A. *EMBO J.* 6:409-417; 1987.
5. Chang, D. D.; Clayton, D. A. *Science* 235:1178-1184; 1978.
6. Chang, D. D.; Clayton, D. A. *Cell* 56:131-1139; 1989.
7. Chu, S.; Archer, R. H.; Zengel, J. M.; Lindahl, L. *Proc. Natl. Acad. Sci. USA* 91:659-663; 1994.
8. Clayton, D. A. *Proc. Natl. Acad. Sci. USA* 91:4615-4617; 1994.
9. Dargemont, C.; Kühn, L. C. *J. Cell Biol.* 118:1-9; 1992.
10. Davis, A. F.; Jeong-Yu, S.; Clayton, D. A. *Mol. Reprod. Dev.* 42:359-368; 1995.
11. Dumont, J. N. *J. Morphol.* 136:153-180; 1972.
12. Dworetzky, S. I.; Feldherr, C. M. *J. Cell Biol.* 106:575-584; 1988.
13. Gold, H. S.; Topper, J. N.; Clayton, D. A.; Craft, H. *Science* 245:1377-1380; 1989.
14. Ho, S. N.; Hunt, H. D.; Horton, R. M.; Pullen, J. K.; Pease, L. R. *Gene* 77:51-59; 1989.
15. Jarmolowski, A.; Boelens, W. C.; Izaurrealde, E.; Mattaj, I. W. *J. Cell Biol.* 124:627-635; 1994.
16. Karwan, R.; Bennett, J. L.; Clayton, D. A. *Genes Dev.* 5:1264-1276; 1991.
17. Kiss, T.; Filipowicz, W. *Cell* 70:11-16; 1992.
18. Kiss, T.; Toth, M.; Solymosy, F. *Eur. J. Biochem.* 152:259-266; 1985.
19. Li, H. V.; Zagorski, J.; Fournier, M. J. *Mol. Cell. Biol.* 10:1145-1152; 1990.
20. Li, K.; Smagula, C. S.; Parsons, W. J.; Richardson, J. A.; Gonzalez, M.; Hagler, H. K.; Williams, R. S. *J. Cell Biol.* 124:871-882; 1994.
21. Lygerou, Z.; Mitchell, P.; Petfalski, E.; Séraphin, B.; Tollervey, D. *Genes Dev.* 8:1423-1433; 1994.
22. Maquat, L. E. *Curr. Opin. Cell Biol.* 3:1004-1012; 1991.
23. Matera, A. G.; Frey, M. R.; Margelot, K.; Wolin, S. L. *J. Cell Biol.* 129:1181-1193; 1995.
24. Mattaj, I. W.; Tollervey, D.; Séraphin, B. *FASEB J.* 7:47-53; 1993.
25. Nigg, E. A.; Bauerle, P. A.; Lührmann, R. *Cell* 66:15-22; 1991.
26. Paluh, J. L.; Clayton, D. A. *Yeast* 11:1249-1264; 1995.
27. Piñol-Roma, S.; Dreyfuss, G. *Nature* 355:730-732; 1992.
28. Riegel, A. T.; Remenick, J.; Wolford, R. G.; Bernard, D. S.; Hager, G. L. *Nucleic Acids Res.* 18:4513-4521; 1990.
29. Schmitt, M. E.; Bennett, J. L.; Dairaghi, D. L.; Clayton, D. A. *FASEB J.* 7:208-213; 1993.
30. Schmitt, M. E.; Clayton, D. A. *Mol. Cell. Biol.* 13:7935-7941; 1993.
31. Schmitt, M. E.; Clayton, D. A. *Genes Dev.* 6:1975-1985; 1992.
32. Schmitt, M. E.; Clayton, D. A. *Genes Dev.* 8:2617-2628; 1994.
33. Simons, F. H. M.; Pruijn, G. J. M.; van Venrooij, W. J. *J. Cell Biol.* 125:981-988; 1994.
34. Terns, M. P.; Dahlberg, J. E. *Science* 264:959-961; 1994.
35. Topper, J. N.; Bennett, J. L.; Clayton, D. A. *Cell* 70:16-20; 1992.
36. Topper, J. N.; Clayton, D. A. *Nucleic Acids Res.* 18:793-799; 1990.
37. Topper, J. N.; Clayton, D. A. *J. Biol. Chem.* 265:13254-13262; 1990.
38. Tyc, K.; Steitz, J. A. *EMBO J.* 8:3113-3119; 1989.
39. Wallace, R. A. *J. Exp. Zool.* 184:321-324; 1973.
40. Yuan, Y.; Tan, E. M.; Reddy, R. *Mol. Cell. Biol.* 11:5266-5274; 1991.
41. Yuan, Y.; Reddy, R. *Biochem. Biophys. Acta* 1089:33-39; 1991.
42. Zasloff, M. *Proc. Natl. Acad. Sci. USA* 80:6436-6440; 1983.